Jump Dynamics and the Isotope Effect in Solid-State Diffusion

M. Marchese, G. De Lorenzi,[a] G. Jacucci,[a] and C. P. Flynn

Department of Physics and Materials Research Laboratory, University of Illinois at Urbana-Champaign, Urbana, Illinois 61801

Vacancy jump rates in fcc solids are calculated accurately on the basis of the short-memory–augmented rate theory. We find that the observed isotope and return jump effects are both dominated by a small temperature-dependent fraction of highly anharmonic trajectories in which strong hard-core interactions occur.

Diffusion rates in solids can be measured to better than 1% in favorable cases. The relative rates for two isotopes can be obtained still more accurately, by a factor of 10, to determine the isotope effect in the atomic jump process.[1] In principle the experimental results contain detailed information about the potential energy and (essentially) classical dynamics of the activated complex during the jump.[2] Unfortunately, no theory has been available to describe, with anything approaching the experimental accuracy, the systematic relationship between the diffusion rate and the potential energy of the relevant atomic arrangements. Indeed, some researchers have concluded that attempts to establish such relationships may not be fruitful.[3] The isotope effect presents a special challenge. Experiments reveal that changes of diffusion rate with the mass of the jumping atom depend largely on the crystal type. Closely similar results are found for all close-packed structures, but no complete explanation has been put forward for the observed behavior.[1] In this Letter we present detailed calculations of vacancy jumps in model crystals that have realistic interatomic potentials. We establish that rate processes can be predicted from first principles with the necessary accuracy when an appropriate theoretical framework is used for the computation. The results demonstrate that core repulsive forces are responsible for dynamical processes that determine the observed isotope effect in single crystals. The methods are equally applicable to other atomic motions in stable solids.

Our results are based on the recently formulated short-memory–augmented rate theory (SM-ART).[4] Certain invariant manifolds of the dynamical system play critical roles in this theory. An interesting and important recent recognition is the way the topology of invariant manifolds constrains the global behavior of dynamial systems in general and, for specific example, in the dynamics of period doubling and the path to chaos.[5] For our present application, the center manifold (CM) in the phase space of the crystal contains all trajectories that oscillate metastably on the potential barrier separating the two crystal configurations between which the atomic jump takes place. This manifold in the SM-ART treatment replaces the "saddle surface" of rate theory[2];

it separates trajectories belonging to the two equilibrium configurations, but in a way which takes correct account of rapid jump reversals due to anharmonic couplings. For a crystal of $N/3$ atoms the CM has $2(N-1)$ dimensions. The $(2N-1)$-dimensional center unstable manifold (CS^-) is derived from the CM by an infinitesimal initial displacement along the direction in which the metastable trajectories decompose; the center stable manifold (CS^+) is the time-reversed analog of CS^-. Figure 1 shows these relationships schematically. The main topological fact of importance here is that any surface Σ drawn from CM to regions of inaccessibly high potential energy cuts all flow lines having one sense; these must pass around CS^+ and CS^-, and are presumed to randomize there, before participating in any return flow.[4] Rapid dynamical events which have the appearance of trajectories with immediate return jumps are separated from Σ by CS^+ or CS^-, and do not contribute to the flux. These dynamical effects cause changes $\sim 10\%$ in defect jump rates even in the least sensitive cases.

Our full-flux calculations for trajectories through Σ proceed as hybrids of theoretical, Monte Carlo (MC), and molecular-dynamics (MD) methods. First, the partition-function integral which determines the probability of the equilibrium crystal configuration (with a vacancy) is compared, by use of difference Monte Carlo
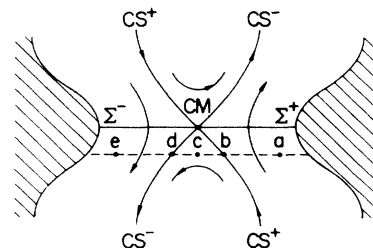

FIG. 1. Sketch of flow lines in phase space showing the center stable (CS^+) and center unstable (CS^-) manifolds and their intersection at the center manifold (CM). Surfaces Σ^+, Σ^- extending from CM to inaccessibly high-energy regions (hatched in figure) cut all the flow in one sense.

methods, with a similar integral for the "saddle plane." In the usual formulation of many-body rate theory,[2] this ratio is the jump rate, apart from trivial factors. The saddle plane S_0 is the hyperplane normal to the unstable mode, at the saddle point of the barrier which inhibits atomic jumps. It is known from MD[6] and explained by SM-ART[4] that the rate at which actual jumps take place falls below the rate at which trajectories cut S_0 in the Vineyard theory.[2] In fact the CM differs from a simple product of saddle-plane and momentum coordinates only because the top of the potential ridge is actually curved with large curvatures, ρ_i^{-1}, along certain principal directions i in the plane.[4,7] We show here that large fluctuations along these principal directions induce hard-core collisions that play a critical role in the isotope effect. This is demonstrated in the second part of our calculation, which proceeds by molecular dynamics. We calculate the fraction of trajectories which cross S_0 but fail to cut Σ. These resemble earlier "conversion coefficient" calculations of Bennett[6] but they use center-manifold concepts as a basis for the true jump criterion. Together, the MC and MD results define the absolute jump rate. We use the Lennard-Jones potential to represent fcc Ar and Morse potentials for fcc Ag and Cu, in crystallites with periodic boundary conditions.

The difference F_m^0 of the free-energy integrals of S_0 and the equilibrium crystal are shown for Ar, Ag, and Cu as functions of T in Fig. 2. The actual figure gives $F_m^0(T)/F_m^0(0)$ as a function of T/T_m, with T_m the melting temperature. Monte Carlo results of runs up to 10^6 steps are indicated by uncertainty bars. These are two-sided samplings[8,9] of the potential-energy difference for the crystal between its equilibrium and saddle-plane configurations, with a chosen mapping from one to the other. The final uncertainties are determined by the observed correlation lengths[9] of several hundred steps that remained even for optimized calculations. Note that direct-difference computations are essential because the free energy of activation is only -1% of the total free energy of the 31-atom periodic clusters.

Curved lines through the points in Fig. 2 represent analytical evaluations of the free-energy differences by anharmonic expansions of the potentials about their extrema[4] and a power-series expansion for the partition functions; the straight lines are the results for harmonic terms only. The relevant expansions take forms like

$$V = V_0 + \tfrac{1}{2}\sum_k \omega_k^2 q_k^2 + V_A, \tag{1}$$

with the q normal coordinates, and with

$$V_A = \tfrac{1}{6}\sum_{ijk} d_{ijk} q_i q_j q_k$$
$$+ \tfrac{1}{24}\sum_{ikrs} e_{ikrs} q_i q_k q_r q_s + \dots. \tag{2}$$

The free-energy difference is[4]

$$F_m^0(T) = F_m^H(T) - (kT)^2(\tilde{A}_1 - A_1) + O(T^3), \tag{3}$$
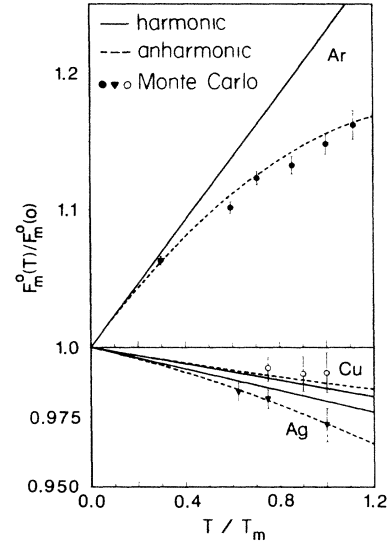

FIG. 2. Free-energy difference (in units of the barrier height) $F_m^0(T)/F_m^0(0)$ between S_0 and the equilibrium state as function of the reduced temperature T/T_m, with T_m the melting temperature.

with

$$F_m^H(T) = -kT \ln\left[\left(\prod_{k=1}^{N-3} v_k e^{-\Delta/kT}\right)\left(\prod_{k=1}^{N-3} \tilde{v}_k\right)^{-1}\right]. \tag{4}$$

$\Delta V = \tilde{V}_0 - V_0$ is the potential-energy difference between the ground and saddle-plane minima and the $v_i = \omega_i/2\pi$ are normal-mode frequencies, with saddle-plane properties distinguished by tildes. Equation (4) is the Vineyard harmonic result but with one extra saddle-point frequency $\tilde{v}_{N-3}$, namely, the frequency along the reaction coordinate in the otherwise frozen ground state. The lines in Fig. 2 are obtained by use of

$$A_1 = \sum_{ijk}(3d_{iik}d_{jjk} + 2d_{ijk}^2)/24\omega_i^2\omega_j^2\omega_k^2$$
$$- \sum_{ik}e_{iikk}/8\omega_i^2\omega_k^2, \tag{5}$$

from Toller et al.[4] and a similar expression with tildes for $\tilde{A}$. It is apparent in Fig. 2 that analytical expressions (curves) reproduce the full MC results for the free-energy difference with an error $<1\%$ for F_m^0 for all three potentials. Thus, the required accuracy in F_m^0 can probably be achieved either analytically from $V(q)$, or by MC methods.

We have employed the identical systems to find what fraction of trajectories that cross the saddle plane actually lead to completed jumps. Given any position on S_0, and velocity in S_0, we have been able to find a perpendicular velocity which causes the trajectory to approach, and linger indefinitely on, the potential barrier; this trajectory (b in Fig. 1) must therefore lie in CS$^+$. Larger velocities (e.g., a) give trajectories leading directly to transitions, and smaller ones (e.g., c) to trajectories

which reverse their perpendicular velocity. Further reductions lead at d to a trajectory which originated at prior time from oscillations near the barrier (i.e., in CS^-) and finally to trajectories (e.g., e) which correspond to jumps in the reverse direction. This sequence is consistent with expected changes from a to e along the broken line in Fig. 1. In practice our calculations proceeded iteratively. A trajectory computed for an estimated initial perpendicular velocity was treated by linear response theory to obtain an improved estimate for use in a subsequent trajectory calculation. The procedure converged rapidly so that only a few iterations were needed. Details will be described in a more complete publication.

The investigation yields values of the critical perpendicular velocity required for a jump, given a position on S_0 and velocity in S_0. All velocities perpendicular to S_0 that are greater than zero would lead to jumps if the potential barrier were not curved. As in Bennett's calculations,[6] the actual fraction Λ of successful jumps is obtained from a probability integral over perpendicular velocities from the critical value (which for our case may be positive or negative) to all higher perpendicular velocities (from b through a to ∞ in the schematic Fig. 1). When averaged over a sampling of initial positions and velocities in S_0, this yields the thermal-average successful fraction $\overline{\Lambda}$. For trajectories near CM the present theoretical framework establishes that the parity of total saddle-plane crossings in a trajectory (odd or even) depends continuously on initial position and momentum coordinates; this assures that crossing rates derived from integrals over states in S_0 and the normal momentum are meaningful (as was simply presumed in the earlier computations[6]).

We have calculated $\overline{\Lambda}$ in three different approximations. The results, presented in Fig. 3, provide interesting comparisons. The line shows the analytical calculations of Toller et al.[4] which use an expansion of the potential up to the first anharmonic terms, viz., the d_{ijk} in Eq. (2). Shown as open circles for the case of Ar are calculations of $\overline{\Lambda}$ obtained from MD by the sampling of trajectories with the anharmonic potential used for the analytical results. The solid circles are MD results for the full crystal potential. The analytical and MD results for the same truncated potential agree precisely. In contrast, the results for the truncated and full potentials differ significantly above $T \sim T_m/4$. The departures that occur at high temperature amount to 5.5% changes of jump rate. These results show that the full MD analysis is essential; the desired accuracy of $\sim 1\%$ cannot be achieved with less effort.

The isotope effect provides a sensitive experimental monitor of the jump dynamics. For the ratio of rates for two isotopes of mass M and $M + \delta M$ one may write[6] $R(M)/R(M + \delta M) = 1 + \kappa \delta M/2M$, with $\kappa = \kappa_H + \overline{\Lambda}^{-1}$ $\times d\overline{\Lambda}/dM$, and κ_H the value of κ for a harmonic approximation to the potential on S_0. Figure 3 shows κ as a
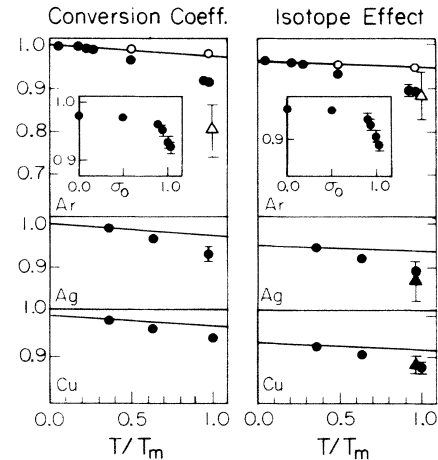

FIG. 3. Analytical anharmonic calculation (solid lines), MD results for the truncated potential (open circles), and MD results for the full potential (filled circles), for the conversion coefficient and the isotope-effect factor for the three models investigated: Ar, Ag, and Cu. Points (open triangles) are values for $\overline{\Lambda}$ and κ computed by Bennett[6] for Ar. Points (filled triangles) are experimental measures of the isotope effect factor from Peterson.[1] Insets: $\overline{\Lambda}$ and κ at T_m for the truncated Ar potential with an added hard-core repulsion, as functions of the core radius σ_0, in units of the Lennard-Jones parameter σ.

function of temperature for our models of Ar, Ag, and Cu, from the analytical method for the truncated potential and MD for the full potential. Experimental results for Ag and Cu are indicated by solid triangles with uncertainty bars. The MD data for the full potential agree with the analytical approximation at low T and are consistent with the experiments near T_m. The overall trend from κ_H at $T = 0$ to the observed κ at T_m is the qualitative behavior suggested much earlier by Flynn.[10]

It is clearly important to understand why the results for the full potentials give very similar κ and Λ as functions of T/T_m while the truncated potentials all give roughly the same wrong answers. By means of additional studies we have established unambiguously that the difference arises from hard-core collisions. Thus, the isotope effect and return jump rate are largely determined by the core repulsion of the full interaction between the moving atom and its neighbors.

We have verified this conclusion in two ways. First, by examining individual MD runs we find that trajectories for the full and truncated potentials are usually very similar. However, in a small, temperature-dependent fraction of events there occur large departures that cause the changes of κ and Λ evident in Fig. 3. These special events correlate with states having large initial values of $Q = \sum_i \varepsilon_i/\rho_i^2$, with ε_i the initial energy associated with direction i in the saddle plane S_0 (with saddle-surface curvature ρ_i^{-1}). In simplified theories[7] the occurrence of rapid return jumps depends on quantities like $\langle Q \rangle$. Motion along those i with ρ_i small is known[7] to create collisions between the migrating atom

and its near neighbors; cases with ε_i large, and consequently Q also large, obviously correspond to strong collisions (Bennett earlier notes the existence of "obstructive" collisions in dynamical simulations[6]). The interpretation is confirmed by the fact that much larger deviations of Λ and κ occur when the velocity is directed to increase the displacement, than in the time-reversed trajectory when the velocity is directed to smaller displacements.

As a check we have performed further calculations in which a rigid core repulsion, of radius σ_0, is added to the truncated potential for Ar. The hard core has little effect for small σ_0 but for values of σ_0 close to unity it causes the reduction of κ shown inset in Fig. 3 (for $\sigma_0 = 1.06\sigma$ the repulsive core occludes the saddle point, σ being the usual Lennard-Jones parameter). Values of σ_0 for the real solid are about 1.02σ,[11] which correctly gives $\kappa \sim 0.89$. These results provide a direct confirmation that the observed effect on κ arises from a deformation of the center manifold associated with the hard-core repulsion. The present calculations are the first to reveal these interesting and general features in the dynamics of atomic jumps in crystals.

In summary, we have described a systematic procedure by which diffusion rates in simple solids may be predicted accurately in terms of the crystal potential. These methods, based on the SM-ART treatment, have been applied to vacancy motion in fcc crystals. A new description of the isotope effect and jump rate at high temperature is obtained. These properties apparently depend on hard-core effects in the crystalline potential. Both the calculated isotope effect and its insensitivity at high temperature to specific atomic forces are in agreement with experiment. The fraction of unrandomized "return jumps" is about 10% for vacancy motion in fcc crystals near T_m.

(a)Present address: Centro del Consiglio Nazionale delle Ricerche, e Dipartimento di Fisica, Università di Trento 38050 Povo, Trento, Italy.

[1]N. L. Peterson, in Diffusion in Solids: Recent Development, edited by A. S. Nowick and J. J. Burton (Academic, New York, 1975).

[2]G. H. Vineyard, J. Phys. Chem. Solids 3, 121 (1957).

[3]Effort has focused instead on models with simplified coordinates and fluctuations parametrized by statistical noise. See, e.g., P. Hanggi, J. Stat. Phys. 42, 105 (1986); H. Frauenfelder and P. G. Wolynes, Science 229, 337 (1985).

[4]M. Toller, G. Jacucci, G. De Lorenzi, and C. P. Flynn, Phys. Rev. B 32, 2082 (1985).

[5]For graphic display, see R. H. Abrahams and C. D. Shaw, Dynamics: The Geometry of Behavior (Aerial Press, Santa Cruz, CA, 1983), Vols. 1 and 2; for period doubling see also J. D. Crawford and S. Onohundro, Physica (Amsterdam) 13D, 161 (1984).

[6]C. H. Bennett, Thin Solid Films 25, 65 (1975), and in Ref. 1, and Colloq. Metall. 19, 65 (1976).

[7]G. De Lorenzi, C. P. Flynn, and G. Jacucci, Phys. Rev. B 30, 5430 (1984).

[8]C. H. Bennett, J. Comput. Phys. 22, 245 (1976); G. Jacucci and A. Rahman, Nuovo Cimento 4D, 357 (1984).

[9]G. Jacucci and A. Rahman, Nuovo Cimento 4D, 341 (1984).

[10]C. P. Flynn, Phys. Rev. Lett. 35, 1721 (1975).

[11]L. Verlet, Phys. Rev. 165, 203 (1968).